JOURNAL OF SOLID STATE CHEMISTRY 4, 199–208 (1972)

A Series of Orthorhombic Tin–Tungsten Bronzes

R. STEADMAN, R. J. D. TILLEY, AND I. J. McCOLM

School of Materials Science & Technology, University of Bradford, Bradford, England

Received April 6, 1971

Tin–tungsten bronzes, Sn_xWO_3, with compositions in the range $x = 0.01$ to 0.3 have been prepared. X-Ray and electron diffraction have been used to determine the structures of those materials, and it is shown that the structures form a related series based upon a previously unreported structural motif. Some of the crystals are faulted, and, using the technique of fringe resolution, electron microscopy has shown the nature of the defects. The results suggest that the phases discovered do not have a significant range of stoichiometry.

Introduction

It was recently reported (*1*) that crystals of composition Sn_xWO_3 ($x = 0.3$ to 0.4) had been prepared which possess structures similar to those of the well-known sodium and potassium tungsten bronzes, and, furthermore, that crystals with values of x ranging down to 0.01 had also been prepared which possess a variety of orthorhombic structures not previously known, but which nevertheless retain the appearance and the electrical conductivity characteristics associated with the tungsten bronzes. While that earlier work established that tin tungsten bronzes had clearly been formed, no attempt had been made to elucidate these new orthorhombic structures of low tin content.

X-Ray and electron diffraction investigations have now revealed that the number of orthorhombic structures which may be formed by these bronzes is much larger than was suspected when they were first reported. The electron diffraction patterns of about nine different structures have been recorded, and five of the structures have so far been isolated in crystals large enough for examination by single crystal X-ray techniques. Complete structure determinations are in progress, and the work is at various stages of completion on the structures under examination, but the position has already been reached at which the basic pattern of all the structures is fully understood.

The existence of this relatively large number of structurally related phases in the composition range $Sn_{0.01}WO_3$ to $Sn_{0.3}WO_3$ is a feature which differentiates these materials from the more widely studied alkali-metal tungsten bronzes. These latter compounds are able to tolerate a substantial range of alkali-metal content before structural changes take place. The alkali-metal atoms (or ions) are usually regarded as partially filling tunnels within a host lattice of WO_6 octahedra, linked by corner sharing. The cation nonstoichiometry is then directly related to the extent to which the tunnels are filled, and it would appear that the host structure only needs to rearrange when the filling of the available sites falls outside a fairly wide range.

Considerable interest has been shown in this phenomenon, and possible relationships between the alkali metal content, the structure and the conductivity of these materials have been reported by a number of authors (*2*, *3*). Although no theories are completely successful in accounting for the conductivity of these materials, a band model appears to be partially correct. However, the atomic orbitals contributing to the conduction band have not been determined with certainty, and whether this band is due to delocalization of tungsten orbitals, alkali-metal orbitals, or to a regular sequence of tungsten–alkali-metal orbitals has not yet been decided.

The orthorhombic tin tungsten bronzes described here have typical "bronze-like" electrical properties, which are retained over the whole composition range. Nevertheless, the number of phases found and the way in which the basic structure is modified by the tin content suggest that accommodation of tin nonstoichiometry by tunnel filling is unlikely and that the electrical properties are probably not related

in a simple way to tin content. This paper describes the basic structural pattern of the low tin content orthorhombic tungsten bronzes. Using these structures as guides, the ability of these phases to tolerate variable tin content is discussed.

Experimental

Metallic tin of 99.999% purity, SnO and SnO_2 of Analar grade were used together with 99.95% tungsten and 99.95% WO_3. The weight of materials necessary for the reactions given by Eqs. (1)–(3) for a range of x values from 0.01 to 0.3 were pressed into pellets of about 0.5 g and sealed in silica tubes at pressures less than 10^{-6} mm Hg. The volume of each tube was about 2 cm^3 and the length 6 cm.

$$x\mathrm{Sn} + \mathrm{WO_3} \rightarrow \mathrm{Sn}_x\mathrm{WO_3}. \quad (1)$$

$$x\mathrm{SnO} + (3-x)/3\mathrm{WO_3} + (x/3)\mathrm{W} \rightarrow \mathrm{Sn}_x\mathrm{WO_3}. \quad (2)$$

$$x\mathrm{SnO_2} + (3-2x)/3\mathrm{WO_3} + (2x/3)\mathrm{W} \rightarrow \mathrm{Sn}_x\mathrm{WO_3}. \quad (3)$$

The tubes were maintained at 1100°C for one week, and at the end of this time the bronzes had been formed. Earlier work showed, however, that some structural variety was present among the crystals of each batch, and to avoid this the contents of the tubes were ground, sealed again in silica tubes, and heated for a further three weeks at 1100°C. This treatment produced well-formed crystals up to 1 mm in size, often well faceted, with a high degree of homogeneity both in structure and in external habit. The crystals were blue-purple and opaque, with the exception of those of lowest tin content, which were transparent.

A modification to the preparative method was attempted in order to get rather larger crystals for conductivity and possibly electron microscopy. A small hole about 1 mm diam was made in the top of the silica tube, which was then encapsulated in a much larger tube and the whole evacuated. It was found that large crystal growths occurred around the mouth of the aperture. The size and quality of crystals prepared depends upon the volume of the sample tube, large volume tubes giving bigger crystals.

It was considered reasonable to assume that the composition of the crystals was that of the original mixture, having regard particularly to the homogeneity of the crystalline product. Three specimens analyzed for tin content by Johnson-Matthey confirmed this belief. Work is in hand to find suitable dissolution and analytical techniques for these materials.

Single crystals suitable for X-ray work could be found in all the specimens which were prepared. Thin needles with diam between 0.005 and 0.05 mm were selected in order to minimize absorption, but absorption corrections were also carried out because of the high absorption coefficient of these materials (~1000 cm^{-1}). The X-ray work was carried out on an integrating Weissenberg camera using Cu$K\alpha$ radiation, and intensities were measured by means of a Joyce-Loebl microdensitometer. Computations were carried out and are being continued at the SRC Atlas Computing Laboratory.

Single crystals prepared in the manner described above could not be thinned chemically. Samples suitable for electron microscope examination were prepared by crushing crystallites in an agate mortar to yield a fine powder. This was collected on carbon films. All samples were examined in an AEI EM6G electron microscope operated at 100 kV. Although the preparation technique did not yield large thin areas of material, sufficient crystals had edges thin enough to yield satisfactory micrographs and diffraction patterns. The spacings of lattice fringes were measured directly on the plate using a Joyce-Loebl microdensitometer.

Results and Interpretation

The unit cell dimensions of four members of the series, as determined from Weissenberg photographs, are given in Table I.

It is evident from those dimensions that each of the structures is of considerable complexity, and a complete structure determination of any one of them would be a major undertaking. The complexity arises partly from the size of the unit cells, each of which contains between 480 and 1040 atoms, and partly also from the nature of the structure itself. Each structure contains a recognizable unit of reasonable size (about 50–100 atoms), and several of

TABLE I

LATTICE PARAMETERS IN Å[a]

	a	b	c
5-type	7.125	14 × 3.795	33.24
6-type	7.415	12 × 3.787	20.40
7-type	10 × 3.896	7.372	50.11
8-type	7.373	2 × 28.92	10 × 3.89

[a] The apparent inconsistency in the labelling of the axes is caused by the desirability of adopting the conventional space groups used in International Tables, Vol. I.

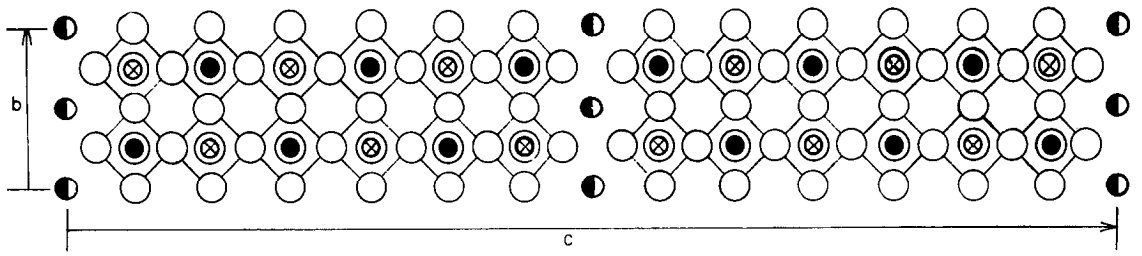

FIG. 1. Projection of 7-type along [100]. The large open circles represent oxygens. The small filled circles are octahedrally coordinated tungstens which are a fractional distance $x = 0.07$ above the paper (which is the b-glide plane). The small circles containing a cross are tungstens at $x = 0.07$ below the paper. The half-filled circles are tins on the b-glide plane.

these units (6–14) are contained within the large unit cell. Among these units there appear to be slight variations in some atomic positions (probably oxygens) to give a large overall repeat distance, and these variations are difficult to determine in the presence of the tungstens. Our purpose at this stage, however, has been to determine the structure of the smaller unit in each case (i.e., with about 50–100 atoms), and the unit cell dimensions given in the following account are submultiples of those of the true unit cells in Table I.

The nomenclature we have adopted to distinguish the members of the series arises partly from the appearance of the X-ray and electron diffraction patterns and partly from the ratio of the longest unit cell dimension to the normal W–W distance in WO_3. The unit cells of all the members are orthorhombic with one very long edge, and from one member to the next in the series the length of this edge changes by one W–W distance. The effect of this is that the diffraction patterns show rows of closely spaced spots, and along any row the nth, $2n$th, $3n$th, etc. spots are much more intense than the rest (though this rule begins to fail at about $4n$ and beyond, because the long cell edge is not an exact multiple of the size of the W–O octahedron which forms the basic unit of structure.) A structure giving such a pattern will be called n-type, and the structures found so far have n values of 5–12, and 19. We shall also refer to, say, the 9-type structure as the 9/18-type, because structure determinations have revealed that although every ninth diffraction spot along a row is strong the long edge of the unit cell is roughly 18 times the W–W separation.

The structures on which X-ray work is in progress will be dealt with individually first of all, followed by those which have so far only been observed by electron microscopy. Since the intention here is to present the over-all picture of this series of structures rather than attempt to give the details of the individual members, crystallographic work will not be described in detail and the measured and calculated structure factors will not be presented, but they will be provided on request; atomic coordinates are represented on the scale diagrams of Figs. 1–4.

7-type $Sn_4W_{24}O_{76}$

This has been more thoroughly examined than any of the others so far. The orthorhombic unit cell has dimensions

$$a = 3.895 \text{ Å}, \quad b = 7.372 \text{ Å}, \quad c = 50.11 \text{ Å}.$$

This lattice is centered on one face, and a glide plane is parallel to this centered face, so the possible space groups are $C2ma$ (= $Abm2$) and $Cmma$. The non-centrosymmetrical $Abm2$ has been used in this investigation. Reflection hkl with $h = 0$–6 were obtained with rotation about the a-axis, and a zero-layer photograph about the b-axis collected the remaining reflections.

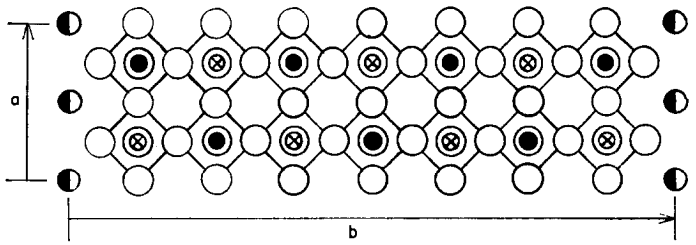

FIG. 2. Projection of 8-type along [001]. See Fig. 1 for key to symbols.

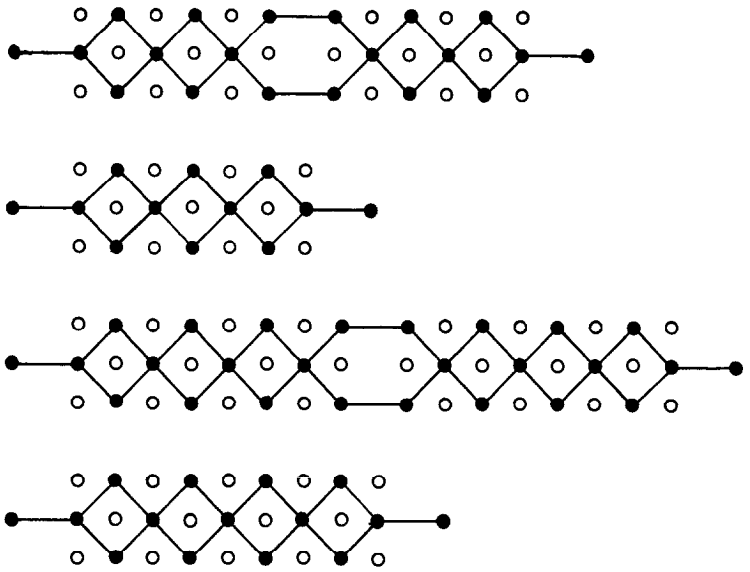

FIG. 3. Framework of tungsten atoms in the structures of 7-, 8-, 9-, and 10-types in order down the page viewed along the shortest axis (3.8 Å). The plane of the paper is a glide plane with the glide component up the page. Filled circles are tungstens just above the paper, and open circles are tungstens below it. Notice that the 7-type and 9-type have unit cells which are slightly less than 14 and 18 normal W–W distances long and are centered on this face.

Three-dimensional Patterson syntheses showed very pronounced peaks corresponding to the W–W and W–Sn vectors, and the superposition technique enabled the heavy atom positions of the model structure given in Fig. 1 to be derived. The oxygens were added in the positions which would be expected, taking into account the normal octahedral coordination of tungsten. The value of R ($= ||Fo| - |Fo||/|Fo|$) obtained without attempt at refinement was 0.25 over 519 observed reflections, showing that the model is basically correct; refinement has reduced this to 0.19, and further work is in progress.

The Fourier syntheses which have been carried out reveal clearly the double layer of tungstens parallel to (100); the two parts of the double layer lie on either side of the *b*-glide plane.

The bulk of the structure is very similar to WO_3 but sliced perpendicular to the *c*-axis into slabs about 20 Å thick, and the interfacial regions between the slabs provide the sites for the Sn atoms. The WO_3 slabs themselves are more symmetrical than crystals of pure WO_3, since the presence of the mirror planes perpendicular to the *b*-axis and the *b*-glide perpendicular to *a* restrict the asymmetry of the WO_3 regions.

It will be of particular interest in a detailed structure analysis to establish the situation of the Sn atoms and their surrounding oxygens. There are four

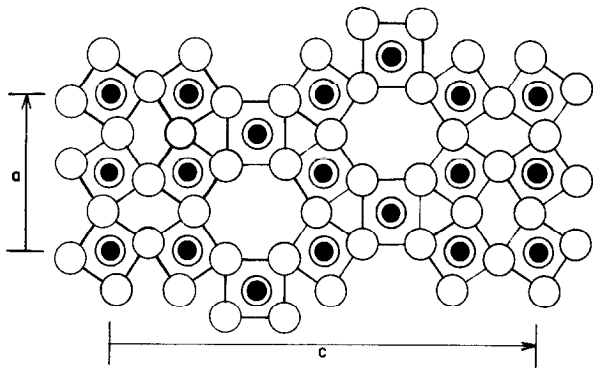

FIG. 4. Projection of 6-type along [010].

Sn in each unit cell, and since the cell extends over two blocks of WO_3, two Sn have z coordinate of zero and the other two are at $z = 0.5$.

8-type $Sn_2W_{14}O_{44}$

Preliminary structure determination has been carried out using only the two-dimensional data $0kl$ and $hk0$. The unit cell dimensions are

$$a = 7.37 \text{ Å}, \quad b = 28.9 \text{ Å}, \quad c = 3.90 \text{ Å}.$$

The cell is primitive with an a-glide perpendicular to the c-axis, so that the possible space groups are *Pm2a* and *Pmma*; the latter has been adopted in this work.

The appearance of the X-ray patterns and the electron diffraction patterns shows that there is a very close similarity between 8-type and the 7-type just described. The similarity is particularly marked in any reciprocal lattice net plane of constant l-value. A centered rectangular pattern (almost square) of intense spots stands out from the rest, and it indicates that a centered rectangular unit approximately 7.5×7.5 Å is a dominant feature of the structure. The same characteristic appearance of the strong reflections is apparent in the patterns of all the structures of 7-type, 8-type, and higher types.

The structure on which refinement is presently to be carried out is shown in Fig. 2. It has been derived from 2-dimensional Patterson syntheses using $hk0$ and $0kl$ reflections, and at this stage the R value over these reflections is 0.25.

The dispositions of the tungstens with respect to the glide plane (in the plane of the paper in these diagrams) is the same in the 7-type and the 8-type structures, and this common feature is brought out clearly in Fig. 3, as is the centered rectangular (square) pattern mentioned earlier.

The 7-type and 8-type provide the key to understanding all the structures of a homologous series of these bronzes. All types higher than these give diffraction patterns which are simply higher variations of 7-type and 8-type patterns, and their structures can be predicted with confidence; Fig. 3 gives the tungsten skeletons of 9-type and 10-type.

6-type $(Sn_{0.17}W)_{10}O_{30}$

The unit cell adopted for the present work has the dimensions

$$a = 7.707 \text{ Å}, \quad b = 3.787 \text{ Å}, \quad c = 20.40 \text{ Å}.$$

In examining any member of this series it is necessary in the early stages to ignore the faint reflections which can only be indexed on the very large cells of Table I. In the case of the 6-type and the 5-type this presents some difficulty, because entire reciprocal lattice net-planes hkl with h odd are composed of faint reflections of this type. If they were to be ignored, the a-axis would be 3.85 Å, but it seemed unreasonable to ignore whole layers of spots completely, so a larger cell ($a = 7.707$ Å) has been used, but no further account has been taken of the faint spots. The structure determination has been carried to its present state, therefore, using only reflections with even h-values.

There is a marked difference between the diffraction patterns of 6- and 5-type on the one hand and those of 7- and higher types on the other. While the most intense spots in the 7-type pattern reveal a centered rectangular subunit in the structure, the prominent spots of the 6-type indicate that the structure contains a hexagonal subunit.

The structure is shown in Fig. 4, and the hexagonal pattern is evident. The heavy atom positions were derived from Patterson syntheses, and oxygens have been added. Some refinement using difference syntheses has been carried out, and the R value over all the reflections employed (i.e., excluding odd h) is 0.17. By ignoring the faint reflections with h odd, ambiguity about the space group is introduced, but the model of Fig. 4 conforms to *Pmma*. The heavy atoms in this structure are situated on a mirror and do not alternate on either side of a glide plane as in 7-type and 8-type.

It is particularly interesting to find that in this structure the tin is only in octahedral coordination, and that the hexagonal tunnels do not appear to provide sites for the tin atoms.

5-type

The unit cell dimensions are

$$a = 33.24 \text{ Å}, \quad b = 3.795 \text{ Å}, \quad c = 7.12 \text{ Å}.$$

Much less work has been carried out on this structure than on those already described, but from a study of the weighted reciprocal lattice a justifiable model can be proposed. The unit cell extends over ten octahedra, even though the appearance of its diffraction pattern leads to its being referred to as 5-type. As with the 6-type, there is clear evidence of a hexagonal subunit, and the lattice dimensions (see Fig. 10) show that the structure is likely to be that of 6-type with a W–O octahedron removed. The structure in Fig. 5 is based on these considerations. The resemblance to the 6-type is clear, and it reflects the similarity of their diffraction patterns.

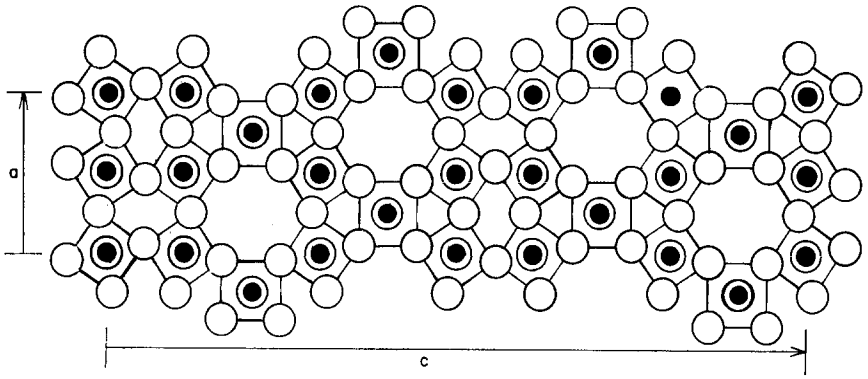

FIG. 5. Projection of a proposed structure of 5-type along [010].

9-type and higher types

These higher types were revealed in the first place by electron diffraction and electron microscopy, and our knowledge of their structure is based principally upon a comparison of their electron diffraction patterns with the X-ray diffraction patterns of lower members of the series. X-ray work has begun on crystals of 12-type.

The electron diffraction patterns of all these higher types resemble very closely the patterns of 7-type and 8-type. The resemblance is so close that to give a description of the structures it is sufficient to state that, as shown in Fig. 3, the members of n-type with n odd are a natural extension of 7-type, and those with n even are simply higher versions of 8-type. The diffraction patterns of 9-type and 10-type are shown in Fig. 6. Examination of the electron diffraction patterns confirms that 9-type and 11-type possess A-centered unit cells and that the c-dimensions extend over 18 and 22 W–O octahedra, respectively. (It is convenient now to use the terms 9/18-type and 11/22-type.)

Care is needed in interpreting the electron patterns of these structures because of the very large unit cells and also because the very faint reflections appear relatively more intense than in X-ray patterns. One pattern, for example, appeared to show the existence of an 8/16-type, which would be anomalous. This can be explained by taking into account the fact that two closely spaced rows of reciprocal lattice spots, which have been identified on the X-ray diffraction patterns, are recorded on one row in the electron diffraction patterns. In this case, spots on the $2k0$ row, taken as an example, showed a spacing corresponding to twice the normal b-dimensions because close to the $2k0$ row was a row of very faint spots which alternated with them.

Faults and Intergrowth Structures

Many of the X-ray photographs taken reveal by the streaking along reciprocal lattice rows that the crystals are faulted, but shed little light on the nature of the faults responsible for the streaks. The large dimensions of the unit cells in these phases is within the resolution limit of the electron microscope, and lattice fringe images have been obtained for all the phases described above. This work has indicated the nature of the faulting which is the cause of streaking on the diffraction patterns.

The majority of crystal flakes examined showed faults in the periodicity of the long lattice spacing. Even in crystals which had been prepared by annealing at 1050°C for 13 weeks, completely fault-free regions, such as shown in Fig. 7, are rare. In such cases the regions of perfect regularity extended over areas of approximately 1 μ square, the largest area which could be photographed at one time, but the true extent of these perfect volumes cannot be estimated. The more usual situation is to see the ordered succession of equally spaced fringes interrupted by fringes that are wider or narrower than the ones regarded as normal. This faulting varies from the isolated faults shown in Fig. 8 to regions approaching a totally disordered state as shown in Fig. 9.

The coherent manner in which isolated faults are linked to the matrix suggests that they are best regarded as lamellae of different bronze types. Making this assumption, the widths of the faults, measured with a microdensitometer, are compared with the lattice parameters of the known bronzes. The long lattice repeat distances of the 5-, 6-, 7-, 8-, and 12-types are known with high accuracy from measurements on Weissenberg photographs; these are plotted in Fig. 10, and interpolated to yield values for the 9-type and higher bronzes. The

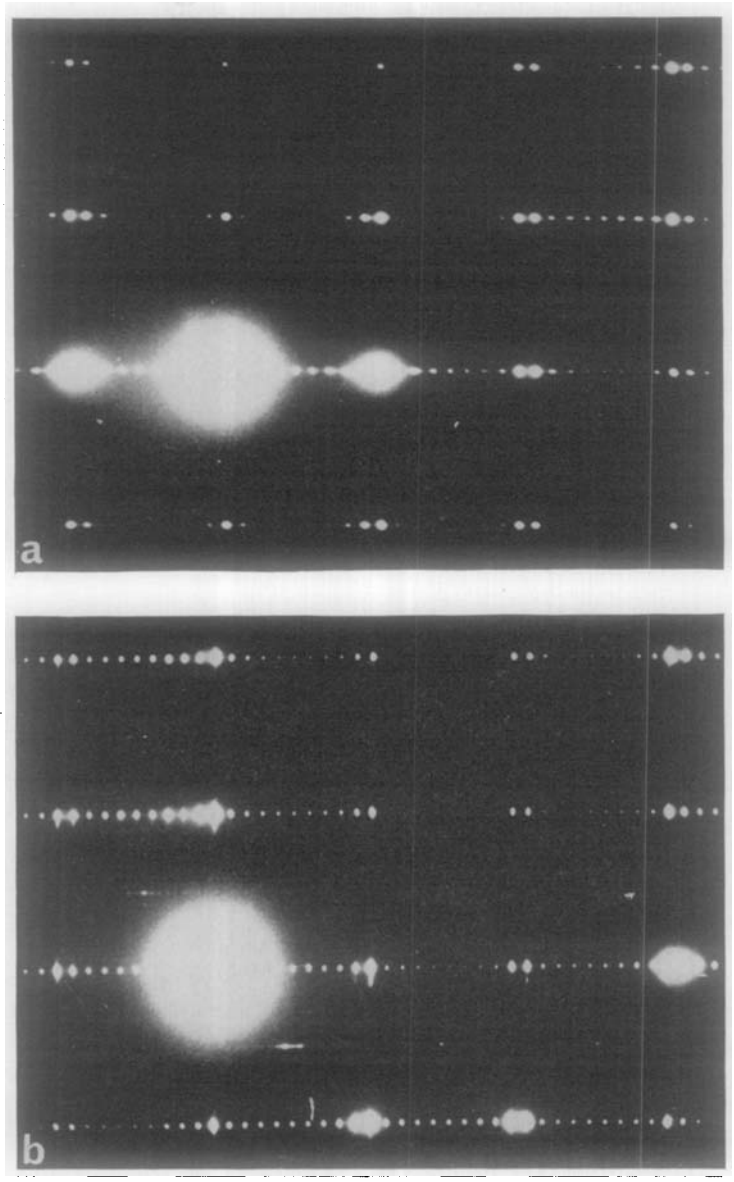

FIG. 6. Diffraction patterns of (a) 9-type and (b) 10-type bronzes. Each row of closely-spaced spots is parallel to the long cell dimension, which is itself perpendicular to the planes containing the tin atoms.

measurement of the widths of isolated faults has an error of between ±5% and ±10%, although for unfaulted material this error is considerably reduced. The error in estimating isolated fault widths is, therefore, of the order of ±1–±2 Å. Because of this limitation the present report restricts the interpretation of faulting to suggesting the likely nature of abnormal lamellae.

The faults shown in Fig. 8 can be taken as an example. The matrix is of the 6-type, as can be seen from the diffraction pattern. The majority of fringes on the micrograph are, therefore, due to the c spacings of the 6-type 20.4 Å. Taking this as a standard, the two wider fringes, C and D in Fig. 8, then correspond to a lattice spacing of 24.5 Å. This figure is taken as confirmation that the faults are indeed due to lamellae of the 7-type bronzes occurring as mistakes in the 6-type crystal. There are also 2 faults A and B which are different from the faults C and D. Fault B has a width of 26.5 Å, and therefore is not 7- or 8-type. This suggests that a new bronze type may exist, or that a lamella of the 7-type is

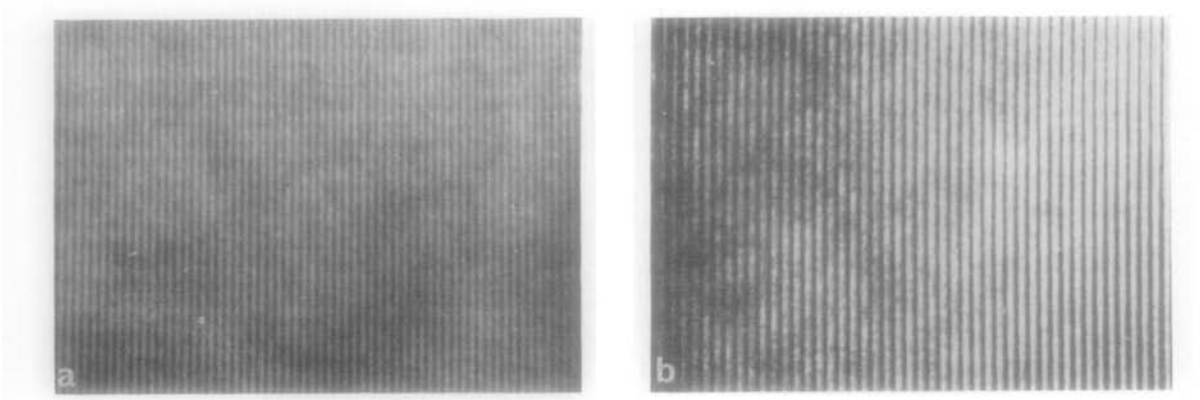

FIG. 7. (a) Ordered lattice fringes of 25 Å spacing, corresponding to the 7-type bronze. (b) Ordered lattice fringes of 32.5 Å spacing, corresponding to the 9-type bronze.

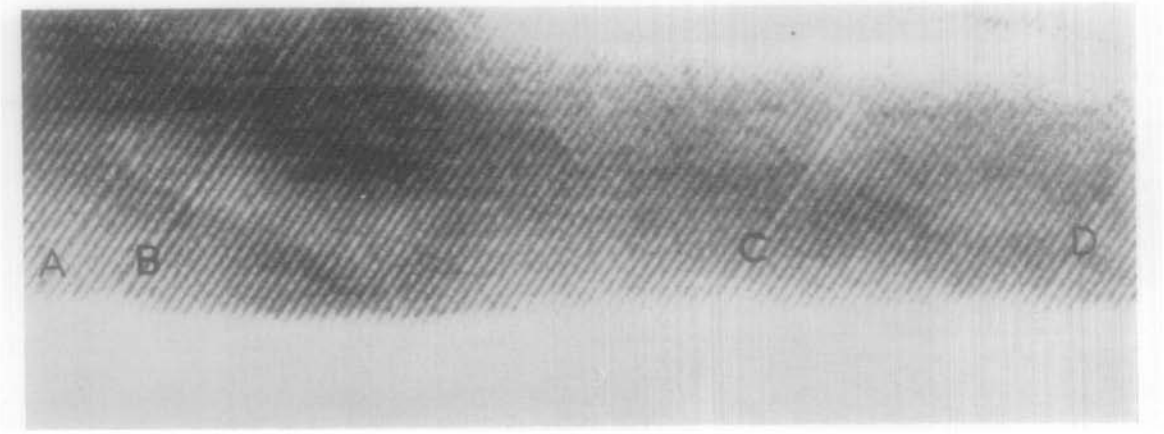

FIG. 8. Isolated faults in a crystal of 6-type bronze. The spacing of the ordered fringes is 20.5 Å. The faults *A* and *B* have spacings not fitting the known bronzes, and the faults *C* and *D* correspond to lamellae of the 7-type bronze (25 Å).

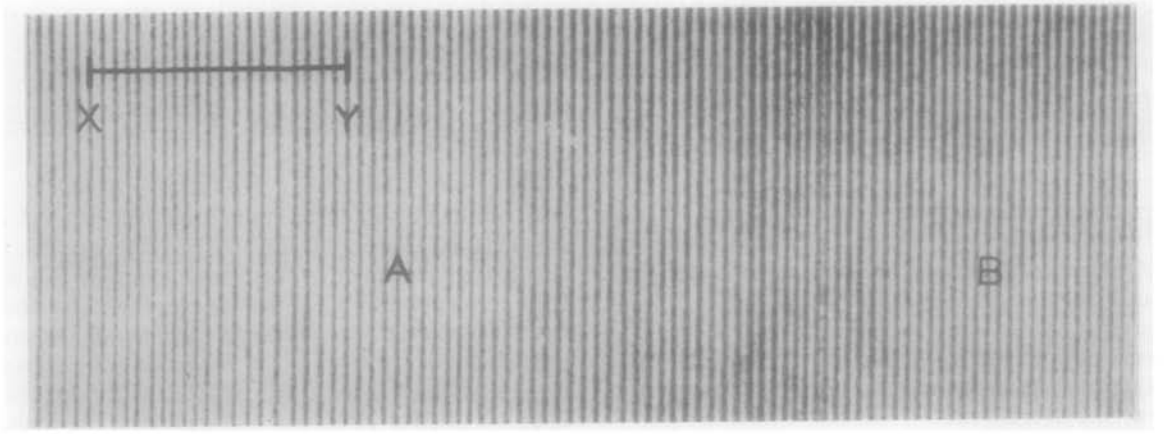

FIG. 9. A faulted crystal of 9-type bronze. The region close to *A* has an ordered set of 32.5 Å fringes corresponding to 9-type bronze, and the region close to *B* has an ordered set of 30 Å fringes corresponding to 8-type bronze. The region *X*–*Y* is disordered and contains 7-, 8-, 9-, 10-, 11- and 12-type spacings.

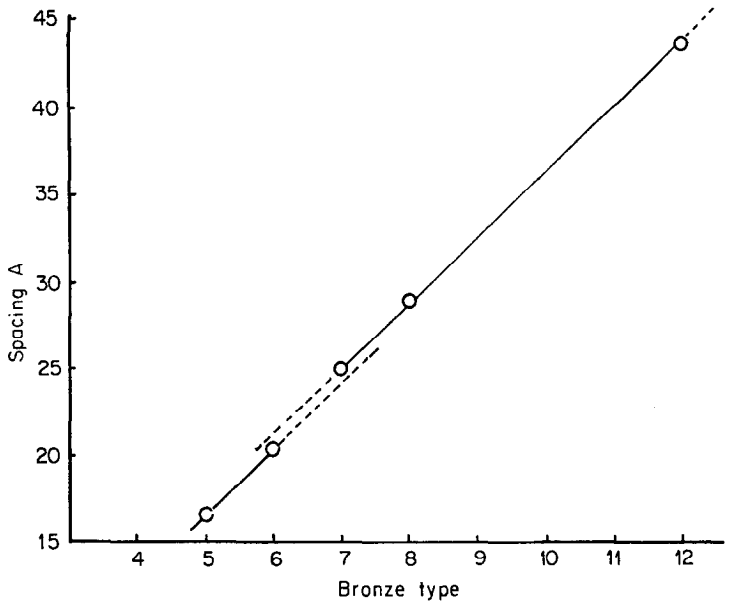

FIG. 10. Variation of the long lattice distance with type of bronze. For the *n*-odd bronzes, this distance has been halved. (See text for details.)

linked to the matrix in a different way from the lamellae *C* and *D*. The fault *A* has a different structure entirely, again suggesting that the linkage is unusual.

The faults shown in Fig. 9 are more in number, and the lattice is correspondingly less regular. The diffraction pattern indicates that the sample is principally of the 8-type, but fainter spots along the lattice rows indicate the presence of a quantity of 9-type. Measurements on the plate reveal these two regions, and the material is, therefore, an intimate mixture of these phases. Some regions of the crystal are severely disordered and appear to be an almost random stack of lamellae of various bronze types. The area *X–Y* in Fig. 9 is an example. It is bounded on either side by regions which are 9-type bronze. An examination of the microdensitometer trace across *X–Y* shown in Fig. 11 reveals that bronze types 7–12 all exist in this area.

Discussion

Two of the members of this series, the 5-type and 6-type, resemble to some extent a Mo–W–O bronze reported by Graham and Wadsley (*4*). All three structures contain hexagonal rings of octahedra, but in the case of the Mo–W–O bronze these form the entire structure, whereas in the 5- and 6-types of the present series the hexagonal formation is interrupted at intervals by octahedra linked almost as in WO_3. This structural difference makes a pronounced and readily recognizable difference between the diffraction patterns, but it may be that further investigation of the tin bronze system will reveal structures of the type found by Graham and Wadsley. They may well exist in the composition range $Sn_{0.2}WO_3$ (6-type) to $Sn_{0.3}WO_3$ (5-type and tetragonal) where structures with pronounced hexagonal features have been observed (*1*).

There are two structural features of the tin bronze series which we have investigated which we consider to be of particular interest not only with regard to these structures themselves but because of the possible implications for other bronze systems. The two features are related in that they are both concerned with the composition range of each member of the series and with the stoichiometry. The first feature is the situation of the Sn ions in the 6-type bronze, and the second is the existence of a large number of structural types within a small range of tin content. We will discuss them in turn.

The presence of the hexagonal tunnels passing through the 6-type (and the 5-type) structure immediately suggests the possibility that these tunnels provide sites for the Sn ions and that the structure may be stable over a wide composition range because the tunnels may be filled to varying degrees. With this in mind the structure factors have been calculated with tin in the tunnel sites, but the effect was a considerable increase in *R* and a pronounced deterioration in the difference syntheses. So, despite the fact that the accommodation of ions

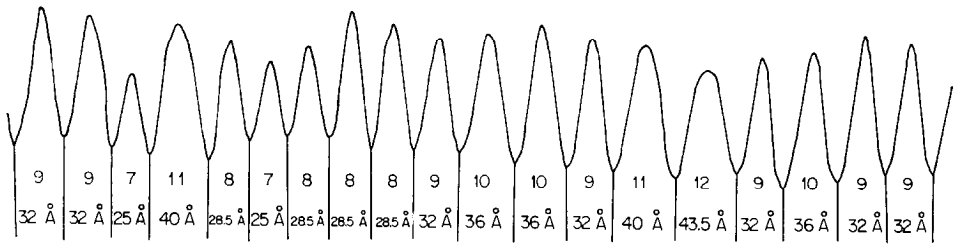

FIG. 11. Microdensitometer trace across the region X–Y in FIG. 9.

in tunnels seems to be a well-established feature of the tetragonal bronzes (*5*, *6*), we can present no evidence in support of it in these orthorhombic structures.

This view of the tin sites is supported by recent detailed Mössbauer investigations. In a previous paper (*1*) the asymmetry of the SnII doublet was ascribed to vibrational anisotropy of the Sn atoms in tunnel sites, but the recent work has revealed that the asymmetry found for bronzes of higher tin content (and therefore tetragonal) probably has a different origin from the asymmetry found in the orthorhombic bronzes of low tin content. The difference of origin is revealed by the difference in temperature-dependence of the asymmetry over the range 4.2–295°K; the bronzes of high tin content ($x > 0.2$) show a much more marked temperature dependence. Accepting the current view that tetragonal bronzes do contain atoms such as tin in tunnel sites, it seems reasonable to suppose that in the orthorhombic bronzes the asymmetry arises instead from some other cause such as the asymmetrical overlap of two or more sets of quadrupole doublets, each arising from a different SnII environment. This indicates either a range of sites within each structure or the presence of several orthorhombic types in the Mössbauer sample. Either of these alternatives would arise if the tin atoms were in octahedral sites and not in tunnel sites.

Turning now to the second feature, the great variety of structures over a narrow composition range, this suggests that none of the structures described is able to accommodate a range of tin compositions. Instead, it would appear that each structure is of fixed stoichiometry, and a change of tin content results in a new, but closely related, structure. The system then can be regarded in the same light as the Ti_nO_{2n-1} oxides (*7–9*) and the Nb_2O_5 and related oxides (*10*) where the supposed variable composition is in fact due to the coexistence of a number of structurally related species. The electron microscope provides direct evidence in support of this interpretation. Consider for example Fig. 9 which shows a type of disorder which is commonly observed. The crystal has grown by vapor deposition, and one can assume that the local concentrations of the vapor species at the growing surface are not likely to fluctuate wildly. If the crystal were able to tolerate a substantial range of stoichiometry, a single phase would be expected, with tin atoms distributed at random in the host structure. However, the micrograph of Fig. 9 makes it apparent that this does not occur; small local composition variations during growth lead to the successive production of lamellae of related bronzes, and this suggests that each type, as it is formed, is not tolerant of compositional variation. Until the locations of the tin atoms within these structures are known with certainty, such considerations must be regarded as speculative. Nevertheless, the results presented here indicate that these orthorhombic bronzes of low tin content are best regarded as line phases.

Acknowledgments

We are indebted to Mr. R. S. Brewerton for Fig. 9, to Professor G. Brown for the provision of microdensitometer facilities, and to the staff of S.R.C. Atlas Computer Laboratory, Chilton, for assistance with the computations.

References

1. I. J. MCCOLM, R. STEADMAN, AND A. HOWE, *J. Solid State Chem.* **2**, 555 (1970).
2. J. B. GOODENOUGH, *Bull. Soc. Chim. Fr.* (**1965**), 1200.
3. M. J. SIENKO, *Advan. Chem. Ser.* **39**, 224 (1963).
4. J. GRAHAM AND A. S. WADSLEY, *Acta Crystallogr.* **14**, 379 (1951).
5. A. MAGNELI, *Arkiv Kemi* **1**, 213 (1949).
6. N. C. STEPHENSON, *Acta Crystallogr.* **18**, 496 (1965).
7. L. JAHNBERG AND STEN ANDERSSON, *Arkiv Kemi* **21**, 413 (1963).
8. J. S. ANDERSON AND R. J. D. TILLEY, *J. Solid State Chem.* **2**, 472 (1970).
9. L. A. BURSILL AND B. G. HYDE, "The Chemistry of Extended Defects in Non-Metallic Solids," p. 347, North Holland (1970).
10. J. G. ALLPRESS, *J. Solid State Chem.* **1**, 66 (1969).